Laplacian filtering: A simple and robust technique for reducing artifacts in Susceptibility Weighted Imaging (SWI)

Ferdinand Schweser[1,2], Andreas Deistung[1], Martin Stenzel[3], Hans-Joachim Mentzel[3], and Jürgen Rainer Reichenbach[1]

[1]*Medical Physics Group, Institute of Diagnostic and Interventional Radiology I, Jena University Hospital - Friedrich Schiller University Jena, Jena, Germany,* [2]*School of Medicine, Jena University Hospital - Friedrich Schiller University Jena, Jena, Germany,* [3]*Section Pediatric Radiology, Jena University Hospital - Friedrich Schiller University Jena, Jena, Germany*

TARGET AUDIENCE – Researchers and clinicians interested in reducing artifacts of susceptibility weighted imaging (SWI), e.g. when applying SWI in the base of the brain.

PURPOSE – Susceptibility weighted imaging (SWI)[1,2] is a novel imaging technique that exploits the MR phase information to delineate venous vessels and brain lesions. The SWI processing involves, first, high-pass filtering of the complex-valued gradient echo (GRE) data (*homodyne* reconstruction) and then, second, multiplicative combination of the filtered complex phase with the magnitude image.[2] As a commercially available imaging technique SWI is established in neuroimaging protocols throughout the world. However, conventional SWI processing is subject to severe off-resonance artifacts due to the strong field gradients induced, e.g., by the air-tissue interfaces above the nasal cavities.[3-6] The high-pass filtering is supposed to eliminate phase wraps (phase aliasing) and large-scale field gradients. However, if the field gradients are too strong, phase wraps can still remain in the filtered image resulting in dark bands in the SWI image (Fig. 1, right column). Various approaches have been presented to avoid these artifacts[3-7]; however, all of these techniques involve rather complex and laborious data processing based on raw complex-valued MR images, which are usually not available in commercial SWI implementations.

In this contribution we present a simple and robust post-processing technique that allows eliminating the wrap-artifacts in SWI. The technique may be applied both retrospectively on filtered phase images (commercial SWI) and prospectively on raw complex-valued images.

THEORY – The wrap-insensitive trigonometric calculus of the Laplace[8] is known to effectively eliminate phase wraps in phase images[9,10]. This calculus may also be used to eliminate residual phase wraps in the high-pass filtered phase images. Two scenarios will be discussed in the following: In the research scenario wrapped complex phase images are available. In this case the Laplacian unwrapping technique may be applied to resolve phase aliasing prior to high-pass filtering. Then, filtering only the unwrapped phase rather than the complex-valued MR image allows attenuating background contributions and, finally, calculation of a wrap-artifact-free SWI. In the commercial scenario only the high-pass filtered phase is usually available with residual phase wraps, and the magnitude images, as in commercial SWI implementations. In this situation, the Laplacian unwrapping may be applied directly to the high-pass filtered phase.

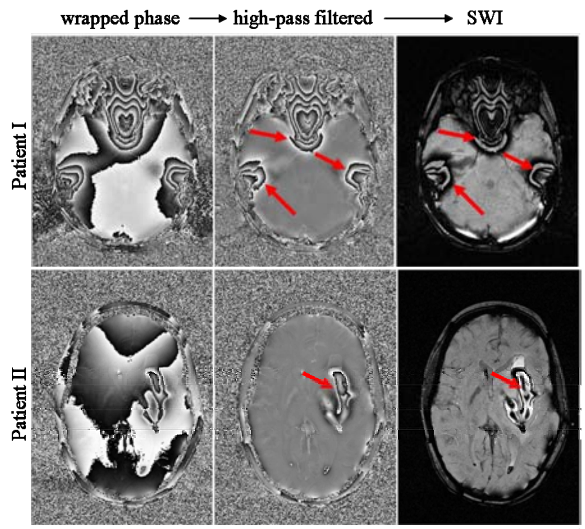

FIGURE 1. Two examples (top and bottom row, respectively) of wrap-artifacts in conventional SWI. **Left**: Raw wrapped phase images (unavailable in commercial SWI). **Middle**: High-pass filtered phase. **Right**: Conventional SWI calculated from the high-pass filtered phase. Arrows mark residual phase wraps in the high-pass filtered phase and wrap-artifacts in the SWI.

METHODS – *Data Acquisition:* Whole-brain data were acquired from 15 pediatric patients (aged 3 years to 15 years, 8 male, 7 female) on a 1.5 Tesla whole-body MRI scanner (Magnetom Sonata and Magnetom Vision, Siemens Medical Solutions, Erlangen, Germany) using a single-channel receive head coil. A fully flow compensated 3D gradient echo (GRE) sequence was applied with the following sequence parameters: TE=40 ms, TR=60 ms, FA=25°, BW=60 Hz/px, $0.5\times0.5\times2$ mm³ image resolution, and 75% partial Fourier along phase and slice encoding direction. *Processing:* For all patients the two situations described in the Theory section were simulated: For the research scenario, the Laplacian unwrapping was applied to the wrapped phase images followed by high-pass filtering of the resulting images using a 32×32 Hanning-window[11] and four-fold multiplication of the resulting images into the magnitude image using a positive phase mask[11]. To mimic the commercial scenario the complex-valued MR data were high-pass filtered using a 32×32 Hanning-window. Subsequently, Laplacian unwrapping was applied to the high-pass filtered phase images, the resulting image was again high-pass filtered and the resulting phase was combined with the magnitude as described above. Processing was performed on a conventional workstation computer in MATLAB (2011b) with a computation time below one minute.

RESULTS – The figures exemplarily show images from two representative patients (I and II). Figure 1 shows the raw wrapped phase images (left; unavailable on commercial SWI implementations), the conventional high-pass filtered phase image (middle), and the SWI magnitude image (right) calculated based on the high-pass filtered phase and the magnitude images (not shown). Both the high-pass filtered phase and the SWI image suffer from wrap-artifacts inside the hemorrhage (arrows in bottom row) and in the vicinity of air-tissue interfaces (arrows in top row), respectively, due to incomplete elimination of phase wraps. Figure 2 shows results of applying the proposed Laplacian-based processing to the high-pass filtered phase images (commercial scenario, Fig. 1-middle column). Wrap-artifacts in the SWI were successfully resolved, resulting in a hypointense appearance of the hemorrhage (bottom row) and no band-artifacts at the edges of the brain (top row), respectively. Almost identical results were obtained when the Laplacian-based processing was applied to the raw phase images (research scenario; not shown). In this case the SWI images were slightly more homogeneous in normal parenchyma. Similar results were obtained in all other patients.

DISCUSSION AND CONCLUSION – The presented technique enables SWI in regions of the brain that were so far difficult to assess, such as regions above the nasal cavities, close to the petrous portion of the temporal bone or inside and in the vicinity of hemorrhagic brain lesions allowing to identify brain lesions or vascular malformations in these regions. The approach can be applied both in a research scenario, when SWI is reconstructed from raw complex MRI data, and in a commercial scenario where usually only high-pass filtered phase images are available. No loss of image quality or resolution is associated with the processing. Nevertheless, it has to be pointed out, that the proposed technique does not completely resolve the issue of artifacts on SWI images due to strong background gradient fields (hypointensities; arrows in top rows in Figs. 1 and 2), which is still an active field of research[12,13].

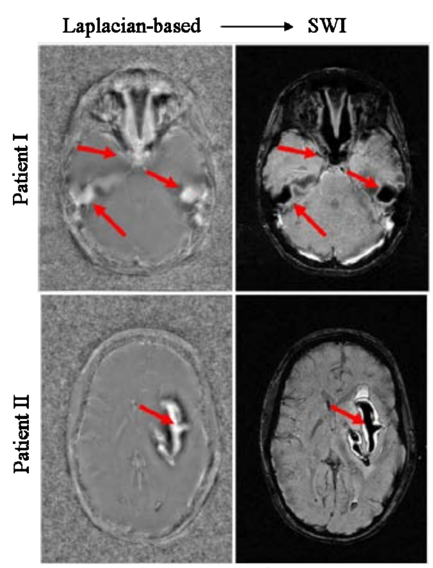

FIGURE 2. Images resulting from the improved SWI processing using the high-pass filtered images in Fig. 1-middle (commercial scenario). **Left**: Image after applying the Laplace and subsequent high-pass filtering. **Right**: SWI calculated from the image in the left column. Arrows point to the same locations as in Fig. 1 marking resolved phase-wraps and suppression of wrap-artifacts, respectively.

REFERENCES – [1] Reichenbach JR et al., 1997. *Radiology*. 204:272–7. [2] Reichenbach JR and Haacke EM, 2001. *NMR Biomed*. 14(7-8):453-67. [3] Jin Z et al., 2011. *J Magn Reson Imaging*. 34(5):1218–25. [4] Denk C and Rauscher A, 2010. *J Magn Reson Imaging*. 31(1):185–91. [5] Ishimori Y et al., 2009. *Acta Radiologica*. 50(9):1027–34. [6] Jin Z et al, 2008. *J Magn Reson Imaging*. 28(2):327-33. [7] Neelavalli J et al., 2009. *J Magn Reson Imaging*. 29(4):937–48. [8] Hÿtch MJ et al., 1998. *Ultramicroscopy*. 74(3):131–46. [9] Schofield MA and Zhu Y, 2003. *Optic Lett*. 28(14):1194-6. [10] Schweser F et al., 2012. *Magn Reson Med* (epub). [11] Reichenbach JR et al., 2000. *J Comp Assist Tomogr*. 24(6):949-957. [12] Schweser F et al., 2011. NeuroImage. 54(4):2789-2807. [13] Liu T et al., 2011. *NMR Biomed*. 24:1129-36.